Author/s:
Akkermann, R;Aprico, A;Perera, AA;Bujalka, H;Cole, AE;Xiao, J;Field, J;Kilpatrick, TJ;Binder, MD

Title:
The TAM receptor Tyro3 regulates myelination in the central nervous system

Date:
2017-04-01

Citation:
Akkermann, R., Aprico, A., Perera, A. A., Bujalka, H., Cole, A. E., Xiao, J., Field, J., Kilpatrick, T. J. & Binder, M. D. (2017). The TAM receptor Tyro3 regulates myelination in the central nervous system. GLIA, 65 (4), pp.581-591. https://doi.org/10.1002/glia.23113.

Persistent Link:
https://hdl.handle.net/11343/292383

TITLE:

THE TAM RECEPTOR TYRO3 REGULATES MYELINATION IN THE CENTRAL NERVOUS SYSTEM

AUTHORS:

Rainer Akkermann[1>], Andrea Aprico[2], Ashwyn A. Perera[2], Helena Bujalka[1^], Alistair E. Cole[1], Junhua Xiao[1], Judith Field[1,2], Trevor J Kilpatrick[1,2#], Michele D. Binder[1,2#*]

[1]Department of Anatomy and Neuroscience, University of Melbourne, Parkville, Victoria, Australia. 3010.

[2]The Florey Institute of Neuroscience and Mental Health, 30 Royal Parade (Cnr Genetics Lane) Parkville. Victoria. Australia. 3052.

#These authors contributed equally to this work

>Current address: Department of Neurology, Heinrich-Heine-University, Dusseldorf, Germany, 40225.

^Current address: Jungers Center for Neurosciences Research, Oregon Health & Science University, Portland, Oregon, USA

RUNNING TITLE:

TYRO3 REGULATES CENTRAL MYELINATION

Correspondence:

*Michele Binder, The Florey Institute of Neuroscience and Mental Health, 30 Royal Parade (Cnr Genetics Lane) Parkville. Victoria. Australia. 3052.

mbinder@florey.edu.au

NUMBER OF WORDS: 229 (Abstract), 674 (Introduction), 813 (Materials and Methods) 1532 (Results) 1330 (Discussion), 100 (Acknowledgements) 707 (Legends), 1206 (Bibliography)

NUMBER OF FIGURES AND TABLES: 5 Figures, 0 Supplementary figures, 0 Tables

TOTAL NUMBER OF WORDS: 6591

MAIN POINTS:

Loss of Tyro3 results in delayed developmental myelination and altered myelin wrapping

In vitro experiments suggest a direct effect of Tyro3 on oligodendrocyte myelination

The Erk1/2 pathway is implicated in this Tyro3 mediated effect

KEYWORDS:

Oligodendrocyte, axon wrapping, Gas6

ABSTRACT

Myelin is an essential component of the mammalian nervous system, facilitating rapid conduction of electrical impulses by axons, as well as providing trophic support to neurons. Within the central nervous system, the oligodendrocyte is the specialized neural cell responsible for producing myelin by a process that is thought to be regulated by both activity dependent and independent mechanisms but in incompletely understood ways. We have previously identified that the protein Gas6, a ligand for a family of tyrosine kinase receptors known as the TAM (Tyro3, Axl and Mertk) receptors, directly increases oligodendrocyte induced myelination *in vitro*. Gas6 can bind to and activate all three TAM receptors, but the high level of expression of Tyro3 on oligodendrocytes makes this receptor the principal candidate for transducing the pro-myelinating effect of Gas6. In this study, we establish that in the absence of Tyro3, the pro-myelinating effect of Gas6 is lost, that developmental myelination is delayed and that the myelin produced is thinner than normal. We show that this effect is specific to the myelination process and not due to changes in the proliferation or differentiation of oligodendrocyte precursor cells. We have further demonstrated that the reduction in myelination is due to the loss of Tyro3 on oligodendrocytes, and this effect may be mediated by activation of Erk1. Collectively, our findings indicate the critical importance of Tyro3 in potentiating central nervous system myelination.

INTRODUCTION

The myelin sheath is a specialised membrane that is wrapped around the axonal projections of neurons. In the central nervous system (CNS) this membrane is formed by oligodendrocytes and is essential for the proper functioning of neurons, in order to facilitate saltatory conduction of action potentials along the axon (Rushton, 1951; Fünfschilling et al., 2012; Lee et al., 2012). In demyelinating diseases such as Multiple Sclerosis (MS), oligodendrocytes and the myelin sheath are damaged and lost. Endogenous remyelination does occur in the early stages of MS, but the response is limited and ultimately fails (Franklin and Gallo, 2014). It has been posited that either lack of trophic support, or the presence of inhibitory factors, could contribute to remyelination failure. This impairment could be driven by limitation in the availability of oligodendrocyte progenitors, or by interference with oligodendrocyte differentiation, including selective failure to elaborate new myelin. Such complexity suggests it will be important to unravel the molecular mechanisms underpinning each step in oligodendrocyte maturation, in order to ascertain how best to develop and apply novel therapeutics that target remyelination.

Tyro3, Axl and Mertk (TAM) are receptor tyrosine kinases that are expressed in various tissues, including the immune and nervous systems (Lu and Lemke, 2001). The receptors are activated by two closely related ligands, Gas6 and Protein S (ProS), but with differing affinities, such that Axl is exclusively activated by Gas6, whereas Tyro3 and Mertk are activated by both ligands (Lew et al., 2014; Tsou et al., 2014). We have previously shown that mice deficient in the TAM ligand Gas6 exhibit increased demyelination and delayed remyelination in response to cuprizone challenge (Binder et al., 2008; 2011). Consistent with these results, exogenous Gas6 has the capacity to enhance myelination in co-cultures of dorsal

root ganglion neurons (DRGs) and oligodendrocyte precursor cells (OPCs) of both rat and human origin (Binder et al., 2011; O'Guin et al., 2013) and to increase remyelination in mice following cuprizone challenge (Tsiperson et al., 2010). However, the receptor responsible for transducing the pro-myelinating effect of Gas6 has not been identified.

Tyro3 is widely expressed in the CNS, particularly in developing white matter tracts (Prieto et al., 2000), although its function in the CNS remains largely unknown. In contrast, in the peripheral nervous system, Tyro3 was recently reported to regulate myelin sheath thickness by Schwann cells (Miyamoto et al., 2015). All three TAM receptors are expressed on OPCs, but whereas Axl and Mertk are subsequently absent from the lineage, Tyro3 is highly upregulated on newly formed and mature myelinating oligodendrocytes (Nielsen et al., 2006; Binder et al., 2008; Cahoy et al., 2008) and Tyro3 expression is lost upon genetic ablation of oligodendrocytes (Golan et al., 2008). During experimental demyelination, Tyro3 expression is decreased in a manner coincident with the loss of the myelin component myelin basic protein (MBP) but recovers with the onset of remyelination, indicating that Tyro3 could play an active role in the repair process (Binder et al., 2008; Huang et al., 2010).

We therefore hypothesised that the pro-myelinating effect of Gas6 could be mediated through Tyro3. In order to test this, we studied the role of Tyro3 in myelination using mice deficient in this receptor ($Tyro3^{-/-}$). We have established that, in the absence of Tyro3, oligodendrocytes are unable to normally myelinate axons *in vitro*. In addition, we have found that the addition of Gas6 does not significantly increase the level of myelination induced by Tyro3 deficient oligodendrocytes,

indicating that the pro-myelinating effect of Gas6 is dependent upon Tyro3 expressed on oligodendrocytes. Further, we have also established that the loss of Tyro3 leads to a delay in developmental myelination, and a reduction in the normal thickness of myelin surrounding axons, clearly linking Tyro3 to the normal process of myelination during development. Additionally, we identified extracellular signal-regulated kinase (Erk)1, a protein known to be involved in the regulation of myelination, as a downstream target of the Gas6-Tyro3 axis in oligodendrocytes. Collectively, our results demonstrate that Tyro3 directly enhances myelination by oligodendrocytes, and that this may be mediated in part by signaling via Erk1.

MATERIALS AND METHODS

Animals and reagents

Sprague Dawley (SD) rats were obtained from the Biomedical Science Animal Facility at the University of Melbourne. Tyro3$^{-/-}$ mice (Lu et al., 1999) and Gas6$^{-/-}$ mice (Angelillo-Scherrer et al., 2001) were fully backcrossed onto the C57Bl/6 background. All animal experiments were conducted according to National Health and Medical Research Council guidelines.

All chemicals were obtained from Sigma-Aldrich (St. Louis, MO) unless otherwise noted. Recombinant human Gas6 was a kind gift from Prof. Greg Lemke (Salk Institute for Biological Studies, La Jolla, CA). All cell culture plasticware was purchased from Nalge Nunc International (Rochester, NY). All cell culture media and reagents were purchased from Invitrogen (Carlsbad, CA) unless otherwise indicated.

Purification and culture of mouse OPCs

OPCs were purified from the brains of P5-P7 mice by immunopanning as previously described (Watkins et al., 2008). Purified OPCs were seeded on poly-D-lysine-coated tissue culture plasticware and cultured in modified Bottenstein-SATO medium (Bottenstein and Sato, 1979) containing N-acetyl-cysteine (60 µg/ml), PDGF-AA (10 ng/ml; Peprotec), NT3 (5 ng/ml; Peprotec), forskolin (5 µM), penicillin and streptomycin.

Co-culture of rat DRG and mouse OPCs

DRGs were isolated from P0-P1 SD rat pups and cultured on coverslips coated with poly-L-ornithine and laminin (Life Technologies) in medium containing NGF (100 ng/ml) including cycles of anti-mitotic medium containing 10μM 5-fluoro-2'-deoxyuridine and 10μM uridine for 2-3 weeks. OPCs were seeded onto pre-cultured DRGs directly after isolation, cultured in SATO media overnight and then maintained in a mixture of 50:50 SATO:Neurobasal media with 2% B27, N-acetyl-cysteine (60μg/ml) and D-biotin (10μg/ml). For assessment of myelination, cells were fixed in 4% paraformaldehyde (PFA) for 10min, blocked with 10% FCS and incubated with anti-MBP and anti-neurofilament (MAB381 and AB1987, Merck Millipore, Massachusetts, USA) overnight, followed by incubation with secondary antibodies (AF594 and AF488, Life Technologies, Carlsbad, CA, USA). Myelination was assessed at either 14 days following the addition of OPCs to DRGs to ensure maximum levels of myelination were reached. In experiments assessing the effect of exogenous factors (Gas6) myelination was assessed at 10 days following the addition of OPCs to DRGs, in order to ensure myelination had not reached maximal levels in the absence of Gas6.

Images for analysis were captured at 10x magnification using an upright Zeiss Axioplan fluorescent microscope (Carl Zeiss, Inc. Thornwood, NY, USA). For the quantification of MBP^{+ve} segments, at least 7 random images with comparable axonal density were counted per coverslip. For the quantification of MBP staining intensity, 10x images were captured using a Zeiss Axioplan fluorescent microscope as above, using the same exposure time and white balance for each image. The

colour channel corresponding to the MB immunofluorescence was extracted and converted to grayscale. Mean gray intensity was measured using ImageJ (v1.50i, National Institutes of Health, USA). At least 7 random images with comparable axonal density were collected and measured per coverslip.

Quantification of oligodendrocyte lineage cell number in optic nerve

Mice were anaesthetised and perfused intracardially with phosphate buffered saline (PBS) followed by 4% PFA. Optic nerves were dissected, fixed in 4% PFA for 1 hour, equilibrated in 20% sucrose in PBS at 4°C overnight. Optic nerves were then embedded in optimum cutting temperature compound (Sakura Finetek, Tokyo, Japan) followed by freezing on dry ice. Cryosections (10µm) were then collected and processed for immunohistochemistry. Blocking and subsequent antibody incubations were performed in 10% normal goat serum/0.1% BSA/0.3% triton X-100. Sections were incubated with mouse anti-APC [(CC1) ab16794, Abcam, Cambridge, MA), rabbit anti-Olig2 (AB9610, Merck Millipore, Billerica, MA), rabbit anti-Ki67 (9106, Thermo Scientific, Waltham, MA) and goat anti-PDGFRα (AF1062, R&D Systems, Minneapolis, MN) overnight at 4°C followed by incubation with appropriate fluorophore-conjugated secondary antibodies (Jackson ImmunoResearch, Baltimore, PA). For quantification of cell number, images were captured using a Carl Zeiss Axioplan microscope with a 40x objective. Images from 3 adjacent section were captured for each animal, and the total number of immunoreactive cells counted. Cell numbers are expressed as cells/mm^2.

Western Blot analysis

Cells lysates were separated by SDS-PAGE and transferred to PVDF membranes. Membranes were probed with specific antibodies against p44/42MAPK (Erk1/2,

#9102), phospho-p44/42MAPK (phospho-Erk1/2, #9101), Akt (#9272) and phospho-Akt (#9271S). All antibodies were obtained from Cell Signaling Technology, MA, USA. All blots shown are representative of at least three independent experiments. The optical density value for each band was determined using NIH ImageJ 1.48v.

Transmission electron microscopy

Mice were anaesthetised with sodium pentobarbitone [100mg/kg, (Virbac, New South Wales, Australia)] and transcardially perfused with 4% PFA. Optic nerves were dissected and incubated in Karnovsky's fixative at 4°C overnight. Samples were then treated with 1% osmium-tetroxide in 1.5% potassium ferrocyanide prior to dehydration with increasing alcohol concentration, incubation and embedding in Spurr's resin. Following confirmation of quality and orientation using semi-thin sections (0.5 µm), ultra-thin sections (90 nm) were cut, stained with uranyl acetate and lead citrate, and viewed using a transmission electron microscope (Jeol Ltd., Akishima, Tokyo, Japan). Myelination of axons was assessed close to the chiasm using ImageJ, as previously described (Binder et al., 2011).

Statistical analyses

All statistical analyses were performed as indicated using GraphPad Prism 6 (GraphPad Software, San Diego, CA, USA). Differences between two groups at a single time-point were analysed using Student's *t*-tests, differences between two groups over multiple time-points were analysed using multiple Student's *t*-tests followed by Holm-Sidak correction for multiple testing. Multi-factor experiments

were analysed using 2-way ANOVA with Sidak's *post-hoc* tests. Differences were considered statistically significant with a *p*-value of < 0.05.

RESULTS

Loss of Tyro3, but not Gas6, leads to delayed myelination during development in mice

Given the known role of Gas6 in myelination *in vitro*, and the circumstantial evidence implicating Tyro3 as the TAM receptor likely to transduce this effect, we investigated developmental myelination in mice in which Tyro3 had been deleted (Lu et al., 1999). We isolated optic nerves from both wild-type (WT) and Tyro3$^{-/-}$ animals at various time-points and analysed the number of myelinated axons using electron microscopy. We observed significantly fewer myelinated axons/mm^2 in optic nerves derived from Tyro3$^{-/-}$ mice as compared with WT mice at P7 (12779±803 vs 26219±3706 myelinated axons/mm^2 for Tyro3$^{-/-}$ and WT mice, respectively; $p_{(raw)}$=0.031, $p_{(adj.)}$=0.1186; Fig.1A-B,D). In contrast, there were no differences in the number of myelinated axons/mm^2 later in development (p>0.05, Fig.1C-D,E). To determine if this delay in myelin initiation was an effect of Gas6 signaling via Tyro3, we also examined the number of myelinated axons in the optic nerves derived from WT and Gas6$^{-/-}$ mice from postnatal day 7 (P7) through to aged mice (Fig.1F-I). During the early stages of myelination, at P7 and P10, we observed a trend towards fewer myelinated axons in the absence of Gas6, but this did not reach statistical significance (P7: 27528±4591 vs 40666±5620; P10: 29578±4002 vs 39478±10615 myelinated axons/mm^2 for Gas6$^{-/-}$ and WT mice, respectively; p > 0.05).

Myelin thickness is altered in two white matter regions in the absence of Tyro3

It has previously been demonstrated that Tyro3 expressed on Schwann cells plays a role in regulating the thickness of the myelin sheath in the peripheral nervous system (Miyamoto et al., 2015). We therefore first assessed the thickness of myelin ensheathing optic nerve axons at P7, the time at which we observed reduced numbers of myelinated fibres in the absence of Tyro3. We performed morphometric analysis of the myelinated fibres and plotted the thickness of myelin as a function of axon diameter (Fig.2A). At this early stage of myelination in the optic nerve, in the WT mice the thickness of myelin increases in proportion to increased axon diameter, with the observed range of axonal diameters within the optic nerve consistent with reported literature (Galabova-Kovacs et al., 2008; Edgar et al., 2009; Traka et al., 2010). In contrast, in the absence of Tyro3, myelin thickness was significantly reduced in comparison with WT mice (p=0.032; Fig.2A). In addition to an overall decrease in mean myelin thickness in the absence of Tyro3 (0.177±0.005 vs 0.140±0.007, p<0.0001; Fig.2B), the reduction in the thickness of myelin was proportionally greater for larger diameter fibres (>1µm: mean myelin thickness 0.200±0.007 WT versus 0.159±0.013 Tyro3$^{-/-}$, p=0.0026; Fig.2D) than for smaller fibres (<1µm: mean myelin thickness 0.154±0.007 WT versus 0.127±0.002 Tyro3$^{-/-}$, p=0.0081; Fig.2C).

As we have already demonstrated a reduction in the number of myelinated axons at P7, the observed reduction in the thickness of myelin surrounding axons at P7 could be either a direct effect of the loss of signaling via Tyro3, or an indirect effect, due to a delay in initiation of myelination. To distinguish between these possibilities, we extended our morphometric analysis to 3 month old mice; at this time the number of myelinated axons was similar between WT and Tyro3$^{-/-}$ mice (Fig.1E). We found that

in the absence of Tyro3, and although the number of myelinated axons was comparable to control, myelin thickness remained reduced in comparison to WT (Fig.2E). In contrast to the earlier time-point, the relationship between axon diameter and myelin thickness appears to have been restored, with axons of all diameter showing similar reductions in myelin thickness. We observed an overall reduction in mean myelin thickness (0.144±0.002 WT versus 0.121±0.002 Tyro3$^{-/-}$, p<0.0001; Fig.2F), that was of a similar magnitude for both large fibres (>1µm: mean myelin thickness 0.188±0.003 WT versus 0.164±0.003 Tyro3$^{-/-}$, p<0.0001; Fig.2H) and small fibres (<1µm: mean myelin thickness 0.107±0.001 WT vs 0.0927±0.001 Tyro3$^{-/-}$, p<0.0001; Fig.2G).

We next determined if the loss of Tyro3 affected myelin sheath thickness in other white matter tracts, beyond the optic nerve. We therefore analysed the corpus callosum of 3 month old Tyro3$^{-/-}$ mice and littermate controls using EM. Consistent with the findings in the optic nerve, we found a significant alteration in the thickness of myelin ensheathing axons in the corpus callosum (p=0.0185, Fig.2I). However, unlike the optic nerve, the Tyro3 dependent alteration in myelin thickness was discordant across different axonal diameters, such that in the Tyro3$^{-/-}$ mice larger axons (>1µm) exhibited a reduction (0.152±0.003 WT versus 0.140±0.004 Tyro3$^{-/-}$, p=0.0171, Fig.2L) but smaller axons (<1µm) exhibited an apparent increase in myelin thickness (0.114±0.001 WT versus 0.119±0.001 Tyro3$^{-/-}$, p=0.0003, Fig.2K).

Tyro3 deletion does not alter the number of oligodendrocyte lineage cells

We next determined whether the reduction in the number of myelinated axons in the absence of Tyro3 was related to alterations in the proliferation or differentiation of

oligodendrocyte precursor cells (OPCs). We therefore examined the number, maturation stage and proliferation of oligodendrocyte lineage cells in optic nerves derived from WT and Tyro3$^{-/-}$ mice at P7. We did not observe any differences in either the total number of PDGFRα^{+ve} OPCs (p>0.05, Fig. 3A-C), or in the proportion of these cells expressing the proliferation marker Ki67 (p>0.05, Fig. 3A,B,D), suggesting that neither the proliferation nor the survival of OPCs in the optic nerve is affected by the loss of Tyro3. The number of CC1^{+ve} mature oligodendrocytes was also similar in WT and Tyro3$^{-/-}$ optic nerves at P7 (p>0.05; Fig. 3E-G). In combination, these data indicate that Tyro3 is involved in the elaboration of myelin by oligodendrocytes, independent of any effect upon the number or proliferation of OPCs, or the number of mature oligodendrocytes.

Loss of Tyro3 results in a reduced capacity of oligodendrocytes to myelinate axons *in vitro*

The developmental delay observed in myelination in the absence of Tyro3 could either be a direct result of the loss of Tyro3 on oligodendrocytes, or an indirect effect of the loss of Tyro3 on other cell types such as neurons, a subset of which are known to express Tyro3. In order to distinguish between these possibilities, we employed an *in vitro* system, co-culturing WT dorsal root ganglia (DRG) neurons with OPCs derived from either Tyro3$^{-/-}$ or WT mice. We observed significantly fewer MBP^{+ve} segments when DRGs were cultured with OPCs from Tyro3$^{-/-}$ mice as compared to WT (21.00±1.11 vs 149.10±19.60 MBP^{+ve} segments/field for OPCs derived from Tyro3$^{-/-}$ and WT mice, respectively; p=0.0004) (Fig. 4A,B). In addition to quantification of myelin segments, we also measured overall expression of MBP in these co-cultures. We detected expression of MBP in co-cultures of DRGs with

OPCs derived from either WT or Tyro3$^{-/-}$ mice, indicating the latter are capable or differentiating into mature MBP^{+ve} oligodendrocytes. However, the overall level of MBP expression is significantly lower in co-cultures of DRGs with Tyro3$^{-/-}$ OPCs compared with WT OPCs (Fig. 4C, p=0.0014). Of note, this decrease in the number of myelin segments occurred in the absence of any reduction in the viability of OPCs derived from Tyro3$^{-/-}$ mice (data not shown).

As we have previously shown that exogenous Gas6 increases myelination in this system, we wished to determine whether this effect was dependent upon Tyro3 expressed upon oligodendrocytes. We therefore examined the effect of adding exogenous Gas6 (100ng/ml) to the co-culture system and compared the extent of myelination by oligodendrocytes derived from either WT or Tyro3$^{-/-}$ mice. Consistent with the data obtained above, there was an overall significant reduction in the number of MBP^{+ve} segments per field in the absence of Tyro3 expression on oligodendrocytes (p=0.002, Fig. 4D). Further, the addition of exogenous Gas6 to Tyro3$^{-/-}$ oligodendrocytes did not significantly increase the number of MBP^{+} segments in these co-cultures (35.13±13.53 vs 39.50±12.92 MBP^{+ve} segments/field without or with 100ng/ml Gas6, respectively; p=0.94) (Fig. 4D). Conversely, the addition of Gas6 significantly increased the number of MBP^{+ve} segments in cultures with oligodendrocytes derived from WT mice (57.29±25.41 vs 87.52±37.10 MBP^{+ve} segments/field without or with 100ng/ml Gas6, respectively; p=0.043). These results indicate that, consistent with the effect of Tyro3 upon the initiation of myelination *in vivo,* Tyro3 regulates myelination of axons *in vitro*, that this effect is mediated through the expression of Tyro3 on oligodendrocytes, and that the pro-myelinating

effect of exogenous Gas6 is dependent upon Tyro3 expressed upon oligodendrocytes.

The Gas6/Tyro3 axis alters Erk1 activation in oligodendrocytes *in vitro*

We next investigated potential downstream targets in oligodendrocytes involved in the pro-myelinating effect of the Gas6/Tyro3 axis. Both Erk signaling (Ishii et al., 2012) and Akt signaling (Flores et al., 2008) constitute major pathways that control myelination. To determine whether Gas6/Tyro3 activity alters these pathways we purified OPCs from both WT and Tyro3$^{-/-}$ mice, which were then differentiated into mature oligodendrocytes *in vitro*, and stimulated with exogenous Gas6 (100ng/ml). Unstimulated cultures were used to test for baseline differences in activation. To assess the activation of each pathway, we determined the relative level of phosphorylated Erk1, Erk2 and Akt compared with the total level of each protein via Western blotting. We found that the relative level of Erk1 phosphorylation was significantly reduced in Tyro3$^{-/-}$ oligodendrocytes compared with WT oligodendrocytes, either in the presence or absence of Gas6 stimulation (no Gas6: 0.56±0.11 vs 0.34±0.06; 100 ng/ml Gas6: 0.79±0.15 vs 0.55±0.01 ratio pErk1/Total Erk1 WT or Tyro3$^{-/-}$ oligodendrocytes, respectively, $p=0.048$) (Fig.5A,B). In contrast, the activation of Erk2 or Akt was not significantly altered by the loss of Tyro3, or by stimulation with Gas6 ($p>0.05$, Fig. 5A,C,D).

DISCUSSION

In this study, we have shown that Tyro3 is involved in the regulation of myelination both *in vitro* and *in vivo*. We observed significantly fewer myelinated axons as well as reduced myelin thickness in the absence of Tyro3 during the initial stages of

myelination within the mouse optic nerve. The number of myelinated axons in Tyro3$^{-/-}$ mice ultimately recovered to WT levels, but myelin thickness remained significantly reduced in adult mice. We have also shown that oligodendrocytes isolated from Tyro3$^{-/-}$ mice produced significantly fewer myelin segments, as compared with oligodendrocytes from WT mice, and that these effects are potentially mediated through Erk1, an intracellular signaling molecule known to be involved in myelination, as a potential downstream target of Tyro3 activation in oligodendrocytes. Collectively, these data indicate a crucial role for Tyro3 in oligodendrocyte induced regulation of CNS myelination.

The development of therapeutic approaches to improve remyelination efficiency in demyelinating diseases such as MS requires an understanding of the mechanisms and pathways that orchestrate myelination. Recent studies investigating the role of the TAM receptor ligand Gas6 have demonstrated that signaling through the TAM family of receptors is important in regulating myelination (Binder et al., 2008; Tsiperson et al., 2010; Binder et al., 2011; O'Guin et al., 2013; Gruber et al., 2014). As unselective activation of all three TAM receptors could have off target effects, it is crucial to identify the principal receptor that transduces the pro-myelinating effects of Gas6, thereby enabling therapeutic strategies to be invoked which target that molecule. Our results demonstrate significantly delayed initiation of myelination during development in the absence of Tyro3 but only a trend towards a defect in the absence of Gas6, suggesting compensation for the loss of this ligand, most likely by the other cognate ligand for the TAM receptors, Protein S (ProS). Concordant with this view, Tyro3 has been shown to be specifically activated by ProS (Stitt et al., 1994; Godowski et al., 1995; Prasad et al., 2005; Lew et al., 2014). Further, in other

contexts, such as phagocytosis of photoreceptors, ProS can fully compensate for the loss of Gas6 (Burstyn-Cohen et al., 2012). Therefore, it is plausible that ProS activation of Tyro3 could compensate for the loss of Gas6 during developmental myelination. It has been previously shown in different mouse models that Tyro3 expression is lost during demyelination, whereas its expression recovers with the onset of remyelination and is further upregulated as repair progresses, coincident with the upregulation of myelin genes such as MBP and MOG (Binder et al., 2008; Huang et al., 2010). These observations, together with our current findings that Tyro3 is an important regulator of developmental myelination, suggest it is likely that this receptor also promotes remyelination in response to a demyelinating insult.

Although our *in vivo* data clearly indicate the involvement of signaling via Tyro3 in the initiation of myelination, this could potentially be mediated by Tyro3 expressed on oligodendrocytes or other cell types, including neurons. The spatial and temporal expression profile of Tyro3, with upregulated expression in developing white matter tracts (Prieto et al., 2000), and in mature oligodendrocytes (Cahoy et al., 2008), suggest that the pro-myelinating effect is most likely mediated directly via Tyro3 expressed on oligodendrocytes. This hypothesis is supported by our *in vitro* data demonstrating a profound impairment of the ability of Tyro3-deficient oligodendrocytes to myelinate axons.

In addition to the delay in the initiation of myelination in the absence of Tyro3, we have identified alterations in the thickness of myelin ensheathing axons in both the optic nerve and in the corpus callosum. These observations complement a recently published study in which Tyro3 deficiency was associated with a reduction in the

thickness of myelin produced by Schwann cells (Miyamoto et al., 2015). In combination, these observations indicate that Tyro3 is important for the regulation of both CNS and PNS myelination.

Early in the development of the optic nerve, the reduction in myelin thickness disproportionately affected larger nerves, but by 3 months of age mice displayed an overall reduction in myelin thickness irrespective of axonal calibre. The growth of myelin was also altered in a separate white matter region in the CNS, the corpus callosum. In contrast to the optic nerve, however, Tyro3 deficiency had distinct effects within the adult corpus callosum, whereby large axons demonstrated a significant reduction in myelin thickness whereas small axons exhibited a significant increase in myelin thickness. Although the exact mechanisms underlying this effect remain to be elucidated, there is precedent from other studies to suggest that the control of myelin initiation and growth can differ according to axonal calibre. For example, the loss of the polarity protein Scribble affects initiation of myelination on small diameter axons (Jarjour et al., 2015), whilst mice with double conditional deletion of fibroblast growth receptors (Fgfr)1 and 2 in oligodendrocytes displayed disproportionately thinner myelin in larger calibre axons (Furusho et al., 2012).

What are the potential functional implications of these observations? The deficit in the initiation of oligodendrocyte induced myelination in the absence of Tyro3 was ultimately resolved over the course of normal development, whilst the quantitative reduction in ensheathment was an ongoing defect. Knowledge of the developmental consequence of delayed myelination is limited, although myriad biological pathways could be altered, including learning and memory (reviewed in (Fields et al., 2014)).

Of particular relevance to Multiple Sclerosis, it has been shown that a developmental delay in myelination is associated with a reduced capacity for myelin repair in the adult (Caprariello et al., 2015).

How might Tyro3 function in the regulation of myelination? Previous work by our group and others has implicated Gas6-mediated TAM signaling in the support of oligodendrocyte survival, and this was transduced through Axl (Shankar et al., 2003; 2006; Binder et al., 2008). In current studies we found no differences in the survival of oligodendrocytes from Tyro3$^{-/-}$ mice relative to WT counterparts, likely a reflection of the culture system which supports high cell viability (Binder et al., 2008). We also found no alteration in the total number of PDGFR α^{+ve} OPCs, or in the proliferating proportion of these cells, nor in the number of mature CC1^{+ve} oligodendrocytes. Instead, in the absence of Tyro3, we observed alterations in the phosphorylation of Erk1, a molecule that has previously been shown to enhance the expression of myelin genes (Guardiola-Diaz et al., 2012; Ishii et al., 2012). Specifically, we showed that phosphorylation of Erk1, but not Erk2, was reduced in oligodendrocytes in the absence of Tyro3, and that, in contrast to WT oligodendrocytes, Erk1 phosphorylation was not induced by exogenous Gas6. This uncoupling of the regulation of Erk1 from that of Erk2 is unexpected, as in a number of studies it has been demonstrated that loss of a single receptor is not sufficient to alter myelination (Fyffe-Maricich et al., 2011). Further, mice with an oligodendrocyte-specific double KO of Erk1/2 show no changes in the initiation of myelination in development, at least in the spinal cord, but they fail to upregulate PLP and MBP mRNAs to a normal level and display a reduction in myelin thickness (Ishii et al., 2012). In contrast, in the absence of Tyro3 we observed a defect in both the initiation of myelination, as well

as in the ensheathment of axons. It therefore seems likely that activation of signaling via Tyro3 affects multiple pathways, including but not limited to Erk1 signaling.

Taken together, the results presented in this study reveal Tyro3 to be an important regulator of CNS myelination, particularly of myelin sheath growth. Little is known about the mechanisms underlying the control of the late stages of myelination, particularly in relation to the regulation of myelin wrapping. Identifying the molecules involved in the control of myelin sheath thickness, and understanding their mechanism of action, has clear implications for the development of therapies to promote remyelination in diseases such as MS, where remyelination is known to result in the generation of abnormally thin myelin (Franklin, 2002). It will therefore be important to determine if Tyro3 is also involved in potentiating remyelination after a demyelinating insult.

ACKNOWLEDGEMENTS:

This work was funded by a grant from Multiple Sclerosis Research Australia. RA was supported by a Melbourne International Research Scholarship. We thank Prof. Greg Lemke of the Salk Institute (San Diego) for the kind gift of the Tyro3 knockout mice. We also thank Dr. Sarah Ellis and Dr. Jill Danne of the Peter MacCallum Cancer Centre Microscopy and Histology facility for technical advice and assistance. The Florey Institute of Neuroscience and Mental Health acknowledges the strong support from the Victorian Government and in particular the funding from the Operational Infrastructure Support Grant. The authors declare no competing financial interests.

BIBLIOGRAPHY

Angelillo-Scherrer A, de Frutos P, Aparicio C, Melis E, Savi P, Lupu F, Arnout J, Dewerchin M, Hoylaerts M, Herbert J, Collen D, Dahlbäck B, Carmeliet P. 2001. Deficiency or inhibition of Gas6 causes platelet dysfunction and protects mice against thrombosis. Nat Med 7:215–221.

Binder MD, Cate HS, Prieto AL, Kemper D, Butzkueven H, Gresle MM, Cipriani T, Jokubaitis VG, Carmeliet P, Kilpatrick TJ. 2008. Gas6 deficiency increases oligodendrocyte loss and microglial activation in response to cuprizone-induced demyelination. J Neurosci 28:5195–5206.

Binder MD, Xiao J, Kemper D, Ma GZM, Murray SS, Kilpatrick TJ. 2011. Gas6 increases myelination by oligodendrocytes and its deficiency delays recovery following cuprizone-induced demyelination. PLoS ONE 6:e17727.

Bottenstein JE, Sato GH. 1979. Growth of a rat neuroblastoma cell line in serum-free supplemented medium. Proc Natl Acad Sci USA 76:514–517.

Burstyn-Cohen T, Lew ED, Través PG, Burrola PG, Hash JC, Lemke G. 2012. Genetic dissection of TAM receptor-ligand interaction in retinal pigment epithelial cell phagocytosis. Neuron 76:1123–1132.

Cahoy JD, Ben Emery, Kaushal A, Foo LC, Zamanian JL, Christopherson KS, Xing Y, Lubischer JL, Krieg PA, Krupenko SA, Thompson WJ, Ben A Barres. 2008. A transcriptome database for astrocytes, neurons, and oligodendrocytes: a new resource for understanding brain development and function. J Neurosci 28:264–278.

Caprariello AV, Batt CE, Zippe I, Romito-DiGiacomo RR, Karl M, Miller RH. 2015. Apoptosis of Oligodendrocytes during Early Development Delays Myelination and Impairs Subsequent Responses to Demyelination. J Neurosci 35:14031–14041.

Edgar JM, McLaughlin M, Werner HB, McCulloch MC, Barrie JA, Brown A, Faichney AB, Snaidero N, Nave KA, Griffiths IR. 2009. Early ultrastructural defects of axons and axon-glia junctions in mice lacking expression of Cnp1. Glia 57:1815-1824.

Fields RD, Araque A, Johansen-Berg H, Lim S-S, Lynch G, Nave K-A, Nedergaard M, Perez R, Sejnowski T, Wake H. 2014. Glial biology in learning and cognition. Neuroscientist 20:426–431.

Flores AI, Narayanan SP, Morse EN, Shick HE, Yin X, Kidd G, Avila RL, Kirschner DA, Macklin WB. 2008. Constitutively active Akt induces enhanced myelination in the CNS. J Neurosci 28:7174–7183.

Franklin RJM, Gallo V. 2014. The translational biology of remyelination: past, present, and future. Glia 62:1905–1915.

Franklin RJM. 2002. Why does remyelination fail in multiple sclerosis? Nat Rev Neurosci 3:705–714.

Furusho M, Dupree JL, Nave K-A, Bansal R. 2012. Fibroblast Growth Factor Receptor Signaling in Oligodendrocytes Regulates Myelin Sheath Thickness. J Neurosci 32:6631–6641.

Fünfschilling U, Supplie LM, Mahad D, Boretius S, Saab AS, Edgar J, Brinkmann BG, Kassmann CM, Tzvetanova ID, Möbius W, Diaz F, Meijer D, Suter U, Hamprecht B, Sereda MW, Moraes CT, Frahm J, Goebbels S, Nave K-A. 2012. Glycolytic oligodendrocytes maintain myelin and long-term axonal integrity. Nature 485:517–521.

Fyffe-Maricich SL, Karlo JC, Landreth GE, Miller RH. 2011. The ERK2 mitogen-activated protein kinase regulates the timing of oligodendrocyte differentiation. J Neurosci 31:843–850.

Galabova-Kovacs G, Catalanotti F, Matzen D, Reyes GX, Zezula J, Herbst R, Silva A, Walter I, Baccarini M. 2008. Essential role of B-Raf in oligodendrocyte maturation and myelination during postnatal central nervous system development. J Cell Biol 180:947-955.

Godowski PJ, Mark MR, Chen J, Sadick MD, Raab H, Hammonds RG. 1995. Reevaluation of the roles of protein S and Gas6 as ligands for the receptor tyrosine kinase Rse/Tyro 3. Cell 82:355–358.

Golan N, Adamsky K, Kartvelishvily E, Brockschnieder D, Möbius W, Spiegel I, Roth AD, Thomson CE, Rechavi G, Peles E. 2008. Identification of Tmem10/Opalin as an oligodendrocyte enriched gene using expression profiling combined with genetic cell ablation. Glia 56:1176–1186.

Gruber RC, Ray AK, Johndrow CT, Guzik H, Burek D, de Frutos PG, Shafit-Zagardo B. 2014. Targeted GAS6 delivery to the CNS protects axons from damage during experimental autoimmune encephalomyelitis. J Neurosci 34:16320–16335.

Guardiola-Diaz HM, Ishii A, Bansal R. 2012. Erk1/2 MAPK and mTOR signaling sequentially regulates progression through distinct stages of oligodendrocyte differentiation. Glia 60:476–486.

Huang JK, Jarjour AA, Oumesmar BN, Kerninon C, Williams A, Krezel W, Kagechika H, Bauer J, Zhao C, Evercooren AB-V, Chambon P, ffrench-Constant C, Franklin RJM. 2010. Retinoid X receptor gamma signaling accelerates CNS remyelination. Nat Neurosci 14:45–53.

Ishii A, Fyffe-Maricich SL, Furusho M, Miller RH, Bansal R. 2012. ERK1/ERK2 MAPK signaling is required to increase myelin thickness independent of oligodendrocyte differentiation and initiation of myelination. J Neurosci 32:8855–8864.

Jarjour AA, Boyd A, Dow LE, Holloway RK, Goebbels S, Humbert PO, Williams A, ffrench-Constant C. 2015. The polarity protein Scribble regulates myelination and remyelination in the central nervous system. PLoS Biol 13:e1002107.

Lee Y, Morrison BM, Li Y, Lengacher S, Farah MH, Hoffman PN, Liu Y, Tsingalia A, Jin L, Zhang P-W, Pellerin L, Magistretti PJ, Rothstein JD. 2012. Oligodendroglia

metabolically support axons and contribute to neurodegeneration. Nature 487:443–448.

Lew ED, Oh J, Burrola PG, Lax I, Zagórska A, Través PG, Schlessinger J, Lemke G. 2014. Differential TAM receptor-ligand-phospholipid interactions delimit differential TAM bioactivities. Elife 3:e03385.

Lu Q, Lemke G. 2001. Homeostatic regulation of the immune system by receptor tyrosine kinases of the Tyro 3 family. Science 293:306–311.

Lu QQ, Gore MM, Zhang QQ, Camenisch TT, Boast SS, Casagranda FF, Lai CC, Skinner MKM, Klein RR, Matsushima GKG, Earp HSH, Goff SPS, Lemke GG. 1999. Tyro-3 family receptors are essential regulators of mammalian spermatogenesis. Nature 398:723–728.

Miyamoto Y, Torii T, Takada S, Ohno N, Saitoh Y, Nakamura K, Ito A, Ogata T, Terada N, Tanoue A, Yamauchi J. 2015. Involvement of the Tyro3 receptor and its intracellular partner Fyn signaling in Schwann cell myelination. Mol Biol Cell 26:3489–3503.

Nielsen JA, Maric D, Lau P, Barker JL, Hudson LD. 2006. Identification of a novel oligodendrocyte cell adhesion protein using gene expression profiling. J Neurosci 26:9881–9891.

O'Guin KN, Gruber RC, Raine CS, Guzik HM, Poulos BK, Shafit-Zagardo B. 2013. Gas6 enhances axonal ensheathment by MBP+ membranous processes in human DRG/OL promyelinating co-cultures. ASN Neuro 6:–.

Prasad D, Rothlin CV, Burrola P, Burstyn-Cohen T, Lu Q, de Frutos PG, Lemke G. 2005. TAM receptor function in the retinal pigment epithelium. Molecular and Cellular Neuroscience 33:96–108.

Prieto AL, Weber JL, Lai C. 2000. Expression of the receptor protein-tyrosine kinases Tyro-3, Axl, and mer in the developing rat central nervous system. J Comp Neurol 425:295–314.

Rushton WAH. 1951. A theory of the effects of fibre size in medullated nerve. J Physiol (Lond) 115:101–122.

Shankar SL, O'Guin K, Cammer M, McMorris FA, Stitt TN, Basch RS, Varnum B, Shafit-Zagardo B. 2003. The growth arrest-specific gene product Gas6 promotes the survival of human oligodendrocytes via a phosphatidylinositol 3-kinase-dependent pathway. J Neurosci 23:4208–4218.

Shankar SL, O'Guin K, Kim M, Varnum B, Lemke G, Brosnan CF, Shafit-Zagardo B. 2006. Gas6/Axl signaling activates the phosphatidylinositol 3-kinase/Akt1 survival pathway to protect oligodendrocytes from tumor necrosis factor alpha-induced apoptosis. J Neurosci 26:5638–5648.

Stitt TN, Conn G, Goret M, Lai C, Bruno J, Radzlejewski C, Mattsson K, Fisher J, Gies DR, Jones PF, Masiakowski P, Ryan TE, Tobkes NJ, Chen DH, DiStefano PS, Long GL, Basilico C, Goldfarb MP, Lemke G, Glass DJ, Yancopoulos GD.

1994. The anticoagulation factor protein S and its relative, Gas6, are ligands for the Tyro 3/Axl family of receptor tyrosine kinases. Cell 80:661–670.

Traka M, Arasi K, Avila RL, Podojil JR, Christakos A, Miller SD, Soliven B, Popko B. 2010. A genetic mouse model of adult-onset, pervasive central nervous system demyelination with robust remyelination. Brain 133:3017-3029.

Tsiperson V, Li X, Schwartz GJ, Raine CS, Shafit-Zagardo B. 2010. GAS6 Enhances Repair Following Cuprizone-Induced Demyelination. PLoS ONE [Internet] 5:e15748. Available from: http://dx.plos.org/10.1371/journal.pone.0015748.t001

Tsou W-I, Nguyen K-QN, Calarese DA, Garforth SJ, Antes AL, Smirnov SV, Almo SC, Birge RB, Kotenko SV. 2014. Receptor tyrosine kinases, TYRO3, AXL, and MER, demonstrate distinct patterns and complex regulation of ligand-induced activation. J Biol Chem 289:25750–25763.

Watkins TA, Emery B, Mulinyawe S, Barres BA. 2008. Distinct stages of myelination regulated by gamma-secretase and astrocytes in a rapidly myelinating CNS coculture system. Neuron 60:555–569.

FIGURE LEGENDS

Figure 1. Optic nerves derived from Tyro3$^{-/-}$ mice have significantly fewer myelinated axons as compared with WT. (A-D) Representative electron micrographs of optic nerves from dissected from Tyro3$^{-/-}$ mice and wild-type (WT) littermates. The number of myelinated axons/mm^2 was quantified for postnatal day 7 (P7), P10 and 3 months (3m), as well as aged mice (>1 year) (*n* = 3-5/group) (E). Values are mean ± SEM. (F-I) Representative electron micrographs of optic nerves from dissected from Gas6$^{-/-}$ mice and wild-type (WT) littermates. (J) The number of myelinated axons/mm^2 was quantified for postnatal day 7 (P7), P10 and 3 months (3m), as well as aged mice (>1 year) (*n*=3-5/group). Values are mean ± SEM. Analysed using multiple Student's *t*-tests followed by Holm-Sidak correction for multiple testing, * $p< 0.05$. Scale bar, 10 µm.

Figure 2: Myelin sheath thickness is reduced in the absence of Tyro3. (A) The thickness of the myelin sheath in relation to axon diameter was quantified for individual axons (n=132) in optic nerves derived from P7 mice (*n* = 3-5/group), showing a reduction in myelin thickness in the absence of Tyro3 (p=0.032), with an overall reduction in mean thickness (B) ($p<0.0001$). This reduction was observed in both (C) large diameter axons (>1µm, p=0.0026) and (D) small diameter axons (<1µm, p=0.0081). (E) Quantification of myelin sheath thickness in relation to axon diameter for individual axons (n=3108) in optic nerves derived from 3 month old mice (*n*= 3-5/group), showed a reduction in myelin thickness in the absence of Tyro3 (p=0.0026) with an overall reduction in mean myelin thickness (F) ($p<0.0001$). This reduction was observed in both (G) large diameter axons (>1µm, p=0.0001) and (H) small diameter axons (<1µm, p=0.0001). (I) Quantification of myelin sheath thickness in relation to axon diameter for individual axons (n=1748) in the corpus callosum of 3

month old mice showed an alteration in myelin thickness in the absence of Tyro3 (p=0.0185) (n=3-4 mice/group). (J) Overall mean myelin thickness was not altered (*p*=0.1673), as we observed a reduction in myelin thickness for (K) large diameter axons (>1µm, *p*=0.0171) but an increase in myelin thickness for (L) small diameter axons (<1µm, p=0.0003). Data analysed using linear regression (A, E, I) or Student's *t-test*.

Figure 3. Tyro3 deficiency does not alter numbers of OPCs or oligodendrocytes in optic nerves at P7. Optic nerves were collected from P7 wild type (WT) and Tyro3$^{-/-}$ mice (*n*=5-6/group). (A,B) Representative images of PDGFR α^{+}Ki67^{+} cells. (C) The total number of PDGFR α^{+} cells/mm^2 and (D) the proportion of proliferating PDGFR α^{+} cells/mm^2, were quantified. (E,F) Representative images of CC1^{+} cells. (E) The total number of CC1^{+} cells/mm^2 were quantified. Values are mean ± SEM. Student's *t*-test. Scale bar, 20 µm

Figure 4. Tyro3-deficiency reduces the capacity of oligodendrocytes to myelinate axons *in vitro*. (A) Oligodendrocyte precursor cells (OPCs) were isolated from wild type (WT) or Tyro3$^{-/-}$ mice (*n*=3/group) and co-cultured with rat DRGs for 14 days. At the end of 14 days, cultures were stained for Myelin Basic Protein (MBP; red) and Neurofilament (green). Insets in (A) show representative images of MBP^{+ve} myelin segments. Quantification of the number of MBP^{+ve} myelinated axonal segments/field showed a significantly fewer myelinated segments in co-cultures of rat DRGs with OPCs derived from Tyro3$^{-/-}$ mice compared with WT (B, *p*=0.0004). In a separate co-culture experiment (n=3-4 mice/group), the total level of MBP expression in co-cultures was determined by assessing the mean intensity of MBP immunofluorescence using ImageJ. We observed significantly lower overall

expression of MBP when DRGs were co-cultured with Tyro3$^{-/-}$ OPCs compared with WT OPCs (C, p=0.0014). (D) OPCs were isolated from Tyro3$^{-/-}$ or WT mice and co-cultured with rat DRGs for 10 days in the presence or absence of Gas6 (100ng/ml). We observed a significant increase in the number of MBP^{+ve} segments in response to Gas6 in co-cultures with WT but not Tyro3$^{-/-}$ OPCs (p=0.043). Student's t-test, *p<0.05 **p<0.01, ***p<0.001, Scale bar, 200μm.

Figure 5: Activation of Erk1 is reduced in the absence of Tyro3. (A) Purified oligodendrocytes were stimulated with 100ng/ml rhGas6 for 15 min and levels of Akt, pAkt, Erk1/2 and pErk1/2 detected using Western blotting. Protein bands were quantified by optical density and expressed as ratios of the phosphorylated protein/total protein. Two-way ANOVA with Sidak's *post-hoc* test, *p<0.05. Values are means ± SEM.

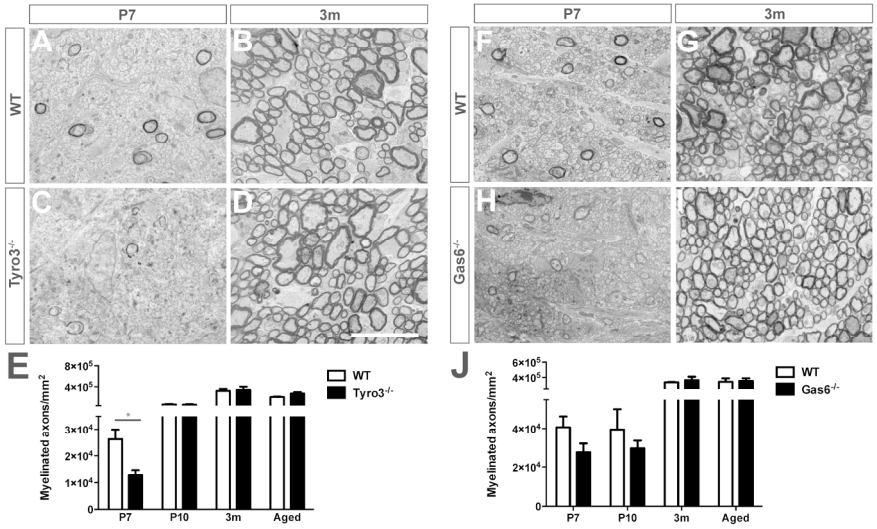

Figure 1

191x110mm (300 x 300 DPI)

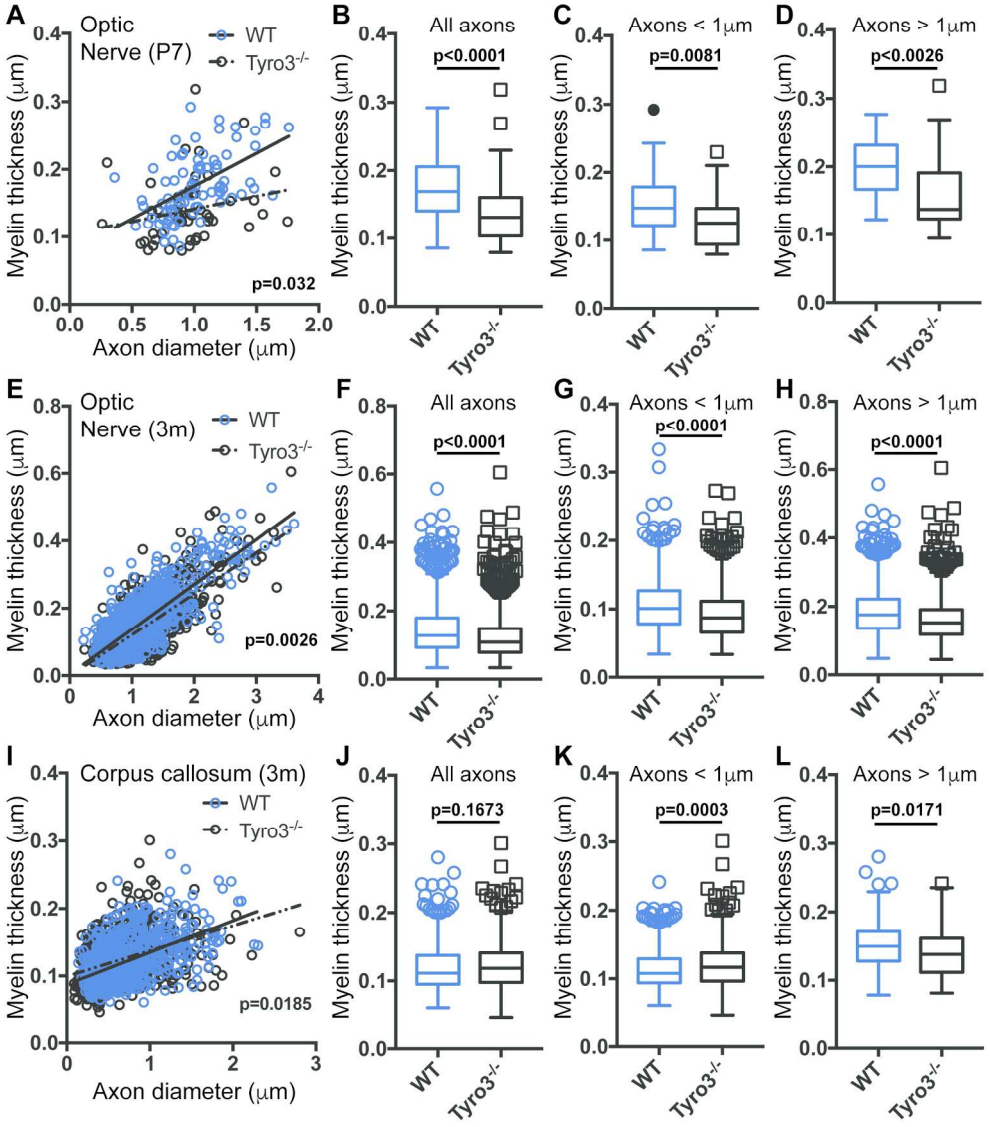

Figure 2

181x220mm (300 x 300 DPI)

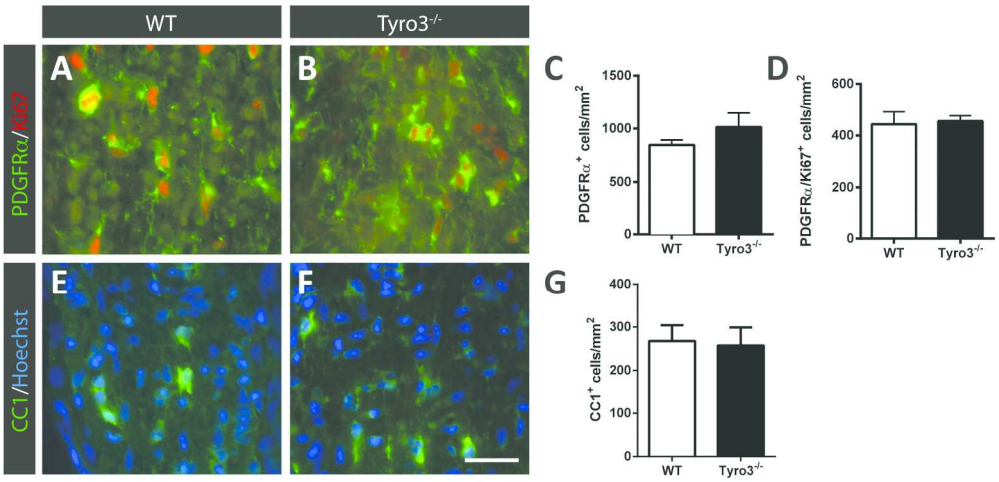

Figure 3

188x89mm (300 x 300 DPI)

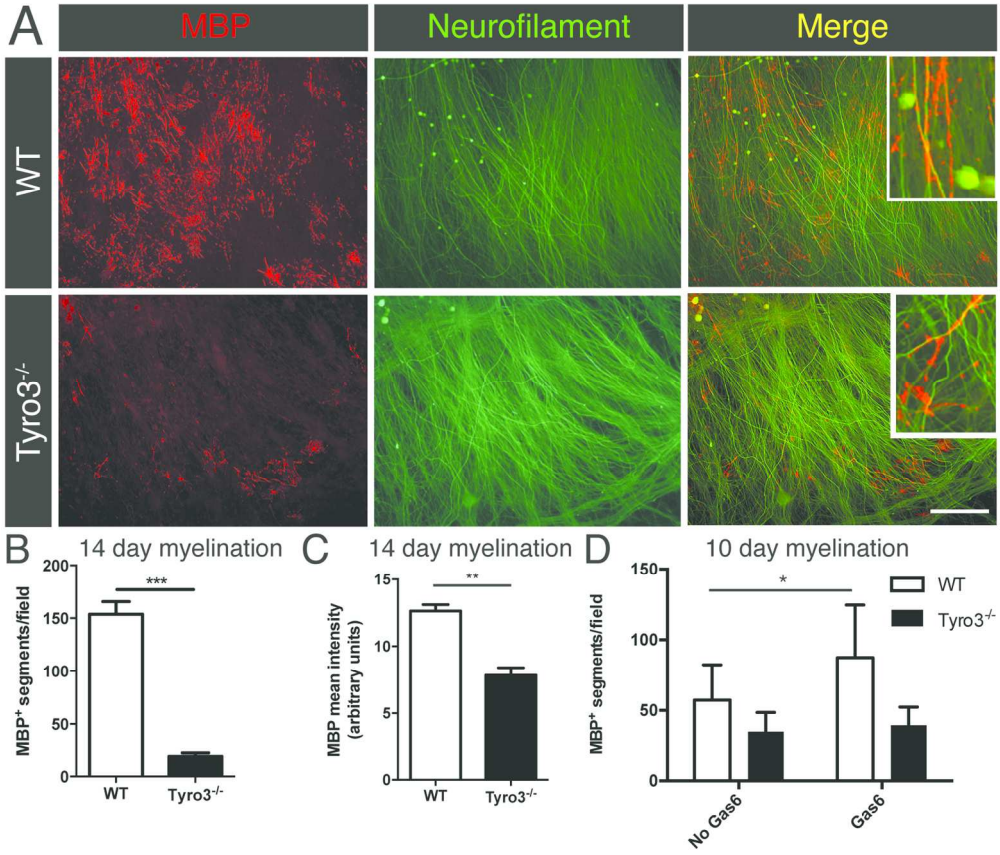

Figure 4

144x124mm (300 x 300 DPI)

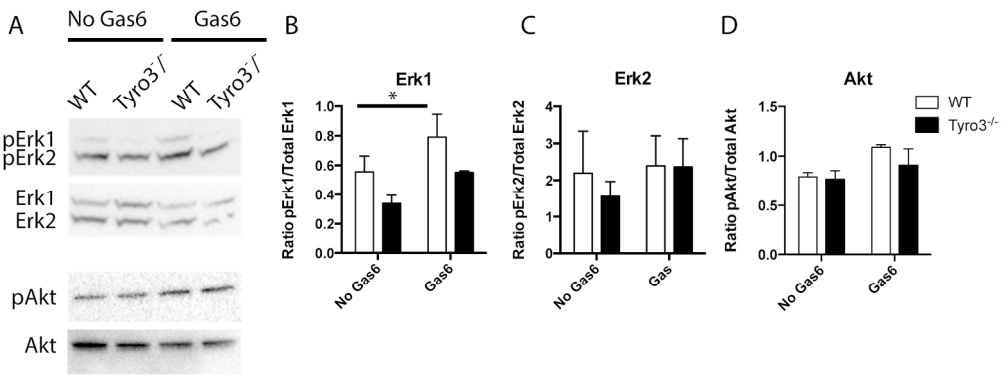

Figure 5

183x67mm (300 x 300 DPI)